Photocatalytic Reactions at Microcrystalline *fac*-Mn(CO)$_3$(η^2-Ph$_2$PCH$_2$PPh$_2$)Cl−Electrode−Aqueous (Electrolyte) Interfaces

John C. Eklund and Alan M. Bond*

Contribution from the Department of Chemistry, Monash University, Clayton, Victoria 3168, Australia

Received March 19, 1999

Abstract: The electrochemical oxidation of *fac*-Mn(CO)$_3$(η^2-dpm)Cl (dpm = Ph$_2$PCH$_2$PPh$_2$) is extensively photocatalyzed when a microcrystal−electrode−aqueous (electrolyte) interface is irradiated with light having a wavelength corresponding to that of the 385 nm charge-transfer band. Investigations of the voltammetry of the solid in the presence and absence of light and monitoring the course of the reaction by EPR, electron probe, and electrochemical quartz crystal microbalance techniques indicate that the catalysis is associated with enhanced charge transport caused by doping of *fac*-Mn(CO)$_3$(η^2-dpm)Cl with photooxidized *mer*-[Mn-(CO)$_3$(η^2-dpm)Cl]X, where the anion, X$^-$, is incorporated into the solid after mass transport from the aqueous electrolyte. Photocatalysis also is found for the electrochemical oxidation of *cis,mer*-Mn(CO)$_2$(η^1-dpm)(η^2-dpm)Br.

Introduction

In recent years, fundamental studies on the voltammetry of solid materials has received much attention[1−10] due to the large number of important applications in fields ranging from novel solar energy devices[11] to molecular electronics.[2,12,13] For example, the voltammetry of mixed valence polyoxotungstate compounds[3−6,10] has been studied extensively and charge transport within the solid has been defined to occur through electron hopping and counterion diffusion mechanisms,[1,2] in contrast to solution-phase voltammetry where the charge is primarily transported by mobile supporting electrolyte ions.[14,15]

In one of the most versatile forms of solid-state electrochemistry,[16−24] redox-active microcrystals are attached to electrode surfaces. The electrode is then placed in an aqueous electrolytic medium in which the microcrystalline material is insoluble. Attachment of solids to an electrode in this manner leads to the formation of an array of microscopically small sites where redox chemistry can take place. As would be expected when an array of microcrystals is attached to an electrode surface, a three-phase electrode/solid/solution boundary is obtained, which allows electrolyte counterions from the solution phase to be transported into or out of the crystal structure upon its oxidation/reduction, to achieve charge neutralization.[17,19]

In solar energy conversion devices, separation of charge in semiconductors occurs upon excitation of an electron from a valence to a conduction band[11,14,15] and this is translated into current flow in an external circuit. In voltammetric studies on solids, charge separation in the crystalline materials usually is generated via application of an external electric field rather that a photolytically induced electron transition. However, there are several examples of organometallic molecules which can be photolyzed by UV/visible light in the solution phase to form a new species in solution that may be oxidized or reduced heterogeneously at an electrode surface. For example, in acetonitrile, the photoelectrochemical oxidation of *fac*-Mn(CO)$_3$-

* To whom correspondence should be sent: E-mail alan.bond@sci.monash.edu.au. Fax: +61 3 9905 4597.

(1) Bruce, P. G., Ed. *Solid State Electrochemistry*; CUP: Cambridge, 1997.

(2) Kulesza, P. J.; Cox, J. A. *Electroanalysis* **1998**, *10*, 73.

(3) Kulesza, P. J.; Faulkner, L. R. *J. Am. Chem. Soc.* **1988**, *110*, 4905.

(4) Kulesza, P. J.; Faulkner, L. R. *J. Electroanal. Chem.* **1988**, *248*, 305.

(5) Kulesza, P. J.; Faulkner, L. R. *J. Am. Chem. Soc.* **1993**, *115*, 11878.

(6) Kulesza, P. J.; Faulkner, L. R. *J. Am. Chem. Soc.* **1991**, *113*, 379.

(7) Parthasatathy, A.; Martin, C. R.; Srinivasan, S. *J. Electrochem. Soc.* **1991**, *138*, 916.

(8) Gorski, W.; Cox, J. A. *J. Electroanal. Chem.* **1992**, *323*, 163.

(9) Jaworski, R. K.; Cox, J. A. *Anal. Chem.* **1991**, *63*, 2984.

(10) Karwowska, B.; Kulesza, P. J *Electroanalysis* **1995**, *7*, 1005.

(11) Pleskov, Y. V. *Solar Energy Conversion, A Photoelectrochemical Approach*; Springer-Verlag: Berlin, 1990.

(12) Chao, S.; Wrighton, M. S. *J. Am. Chem. Soc.* **1987**, *109*, 2197.

(13) Mirkin, C. A.; Wrighton, M. S. *J. Am. Chem. Soc.* **1990**, *112*, 8596.

(14) Bard, A. J.; Faulkner, L. R. *Electrochemical Methods: Fundamentals and Applications*; John Wiley: New York, 1980.

(15) Brett, C. M. A.; Oliveira-Brett, A. M. *Electrochemistry, Principles, Methods and Applications*; OUP: Oxford, 1993.

(16) Bond, A. M.; Cooper, J. B.; Marken, F.; Way, D. M. *J. Electroanal. Chem.* **1995**, *396*, 407.

(17) Bond, A. M.; Colton, R.; Daniels, F.; Fernando, D. R.; Marken, F.; Nagaosa Y.; Van Steveninck, R. F. M.; Walter, J. N. *J. Am. Chem. Soc.* **1993**, *115,* 9556.

(18) Bond, A. M.; Marken, F. *J. Electroanal. Chem.* **1994**, *372*, 125.

(19) Shaw, S. J.; Marken, F.; Bond, A. M. *J. Electroanal. Chem.* **1996**, *404*, 227.

(20) Bond, A. M.; Fletcher, S.; Marken, F.; Shaw, S. J.; Symons, P. G. *J. Chem. Soc., Faraday Trans.* **1996**, *92*, 3925.

(21) Dostal, A.; Meyer, B.; Scholtz, F.; Schroder, U.; Bond, A. M.; Marken, F.; Shaw, S. J. *J. Phys. Chem.* **1995**, *99*, 2096.

(22) Downard, A. J.; Bond, A. M.; Hanton, L. R.; Heath, G. A. *Inorg. Chem.* **1995**, *34*, 6387.

(23) Bond, A. M.; Colton, R.; Marken, F.; Walter, J. N. *Organometallics* **1994**, *13*, 5122.

(24) Bond, A. M.; Colton, R.; Mahon, P. J.; Snook, G. A.; Tan, W. T. *J. Phys. Chem. B* **1998**, *102*, 1229.

(25) Compton, R. G.; Barghout, R.; Eklund, J. C.; Fisher, A. C.; Bond, A. M.; Colton, R. *J. Phys. Chem.* **1993**, *97*, 1661.
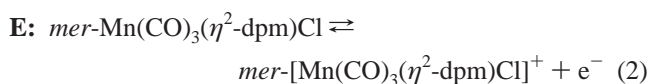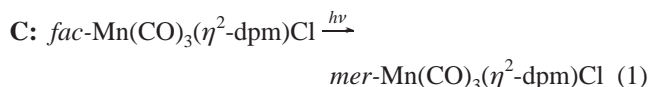
(26) Bond, A. M.; Colton, R.; McCormick, M. J. *Inorg. Chem.* **1977**, *16*, 155.

(27) Bond, A. M.; Grabaric, B. S.; Grabaric, Z. *Inorg. Chem.* **1978**, *17*, 1013.

(28) Colton, R.; McCormick, M. J. *Aust. J. Chem.* **1976**, *29*, 1657.

(29) Carriedo, G. A.; Riera, V.; Santamaria, J. *J. Organomet. Chem.* **1982**, *234*, 175.

(η^2-dpm)Cl, where dpm is $Ph_2PCH_2PPh_2$, occurs via the following photo-CE mechanism:[25]

C: fac-Mn(CO)$_3$(η^2-dpm)Cl $\xrightarrow{hv}$

$$mer\text{-Mn(CO)}_3(\eta^2\text{-dpm)Cl} \quad (1)$$

E: mer-Mn(CO)$_3$(η^2-dpm)Cl $\rightleftarrows$

$$mer\text{-[Mn(CO)}_3(\eta^2\text{-dpm)Cl]}^+ + e^- \quad (2)$$

If mechanisms of these kinds occur in the solid state upon UV/visible irradiation, then the voltammetry of a microcrystalline organometallic material attached to a solid electrode surface can be envisaged to give rise to two prime possible outcomes: (1) As in the case of semiconductor electrodes, charge separation could occur within the microcrystalline environment upon irradiation, resulting in a current flow and concurrent charge balance through diffusion of ions into the crystalline material. (2) The material attached to the electrode could undergo a chemical transformation to form a material within the solid environment that can be oxidized or reduced at a different potential from that of the starting material and hence give rise to a photocatalytic reaction.

In this work, microcrystals of the fac-Mn(CO)$_3$(η^2-dpm)Cl manganese(I) organometallic compound have been attached to an electrode surface and the solid-state photoelectrochemistry of this complex has been investigated. Knowledge of the solution-phase voltammetry[25−27] and the ready accessibility of both Mn(I) and Mn(II) oxidation states suggested that both above-mentioned routes could be available upon photolysis of microcrystals of this compound attached to a solid electrode surface that is in contact with an electrolytic aqueous medium.

Experimental Section

Reagents, Compounds, and Solvents. All electrolytes (NaCl, NaClO$_4$, LiCl, BaCl$_2$, HCl, KCl, NaOH, NaNO$_3$, Na$_2$SO$_4$, and NaF) were of analytical or electrochemical grade purity. Triply distilled water was used for preparation of all the aqueous electrolyte solutions. Dichloromethane and acetonitrile were of HPLC grade (99.9%, Mallinckrodt) and were dried for at least 12 h over molecular sieves prior to use. The chemical oxidant, NOBF$_4$, was used as supplied by Aldrich (Minnesota, WI). Fac-Mn(CO)$_3$(η^2-dpm)Cl[28] and cis,mer-Mn-(CO)$_2$(η^1-dpm)(η^2-dpm)Br[29] were prepared using methods based on standard literature procedures. All solutions were thoroughly purged of oxygen by outgassing with nitrogen that had been presaturated with the appropriate solvent.

Instrumentation and Procedures. Solid-state photoelectrochemical voltammetric experiments were undertaken using in-house fabricated 5 mm diameter pyrolytic graphite disk electrodes housed in a Teflon mount, an Ag/AgCl (3 M KCl) reference electrode, and a platinum wire counter electrode. Small amounts of fac-Mn(CO)$_3$(η^2-dpm)Cl or cis,mer-Mn(CO)$_2$(η^1-dpm)(η^2-dpm)Br crystalline solid were placed on a coarse grade filter paper and the material was ground to microcrystalline size ($\leq$10 μm as determined by electron microscopy; the instrumentation used is described below) using the flat side of a spatula. A cotton bud was then rubbed over the microcrystalline material and adhered solid transferred to the electrode by rubbing the cotton bud end over the electrode surface. Finally, the microcrystal coated electrode was placed into the electrochemical cell which contained an electrolytic aqueous medium. A water-jacketed cell, connected to a Grant Instruments water bath/pump circulating system, was utilized to maintain a constant temperature of (22 $\pm$ 1)°C for experiments with and without irradiation. A quartz disk (Herbert Groiss, Victoria, Australia) was attached to the bottom of the cell to allow unhindered passage of UV/visible irradiation to the electrode surface. The quartz disk was attached to the cell using a spring clip and a good seal was maintained using a rubber "O-ring" between the plate and the cell. All voltammetric

experiments were undertaken with an ADI instruments Maclab/4e potentiostat system controlled by a Macintosh Powerbook microcomputer and potentials are quoted versus the aqueous Ag/AgCl (3 M KCl)-reference electrode.

For photochemical experiments, UV/visible irradiation was provided by a broad band 300 W xenon arc lamp (Cermax LX300; ILC technology, Sunnyvale, CA) enclosed in a R400 lamp holder (ILC technology). The infrared component was removed by an infrared transparent mirror after which the light was passed through a series of lenses and focused into an optic fiber (ILC technology) directed at the surface of the working electrode. The wavelength of the incident light was controlled via a range of UV/visible colored-glass filters (Jena Glaswerk, Schott & Gen., Mainz, Germany). Quantitative voltammetric experiments were conducted using a filter which had a wavelength range of 300−450 nm and yielded an internal transmittance of 50% or above, with 90% transmittance between 350 and 400 nm and less than 1% between 500 and 680 nm. The intensity of this filtered light source was calibrated using the known[25] photoinduced isomerization rate of fac-Mn(CO)$_3$(η^2-dpm)Cl (absorption band of compound centered at 385 nm). Typically intensities of 10 mW cm^{-2} were obtainable in the 300−450 nm UV/visible region. In some experiments a further blue-green filter was utilized which had >95% transmittance between 330 and 550 nm. To obtain action spectra, a sequence of colored glass filters were used for which 50% internal transmittance (ϑ_{50}) occurred at 230, 335, 360, 385, 395, 400, 420, 435, 455, 475, and 550 nm, respectively. The transmittance of these filters rose sharply on moving from lower to higher wavelengths. A rise from 10 to 90% was attained over a 10−40 nm range, the filters allowing >99% transmittance for all wavelengths 40−80 nm greater than the quoted ϑ_{50} values. Thus, an estimate of the minimum wavelength available with the significantly transmitted filtered light could be made.

X-band EPR measurements were made with a Varian E−12 spectrometer. EPR spectra were recorded at 77 and 295 K. Gains in the range 10^3−10^4 and modulation amplitudes of 4.0 G were used.

Simultaneous voltammetric and mass balance experiments were undertaken with an electrochemical quartz crystal microbalance (EQCM) consisting of an Elchema (Postdam, NY) model EQCN-701 nanobalance and model PS-205 potentiostat. The system was controlled by a 486 PC running VOLTSCAN software (Intellect Software, Postdam, NY). The working electrode for the EQCM measurements was one side of a 13 mm diameter AT-cut quartz crystal (Bright Star Crystals, Rowville, Victoria, Australia) that had gold disks (5.0 mm diameter) vapor deposited on each side and oscillated at a frequency of 10 $\pm$ 0.05 MHz. The method of calibration of the EQCM was as described previously.[30] Solid microcrystalline material was attached to the gold electrode surface using the same technique described above for the graphite electrode.

Surface elemental compositions of the manganese compounds attached to a 5 mm diameter pyrolytic graphite electrode were determined by the electron microprobe technique. The instrumentation used for these measurements consisted of a scanning electron microscope (JEOL JSM 840A) coupled to an X-ray analyzer (Moran scientific; 20 KV accelerator voltage). For these experiments, the electrode to which solid had been attached was placed in the aqueous electrolyte solution for 5 min in the absence and then presence of light. The graphite disk electrode was then removed from its Teflon mount, rinsed with distilled water, and fixed with double-sided tape onto a stub and gold plated in a Balzers sputter-coating unit.

Results and Discussion

A. Voltammetry of fac-Mn(CO)$_3$(η^2-dpm)Cl at a Solid−Electrode−Aqueous (0.1 M NaCl) Interface in the Presence and Absence of Light. Initial solid-state voltammetric experiments were conducted at a microcrystalline fac-Mn(CO)$_3$(η^2-dpm)Cl−graphite electrode−0.1 M NaCl aqueous electrolyte interface. In the absence of irradiation with light, repeated cycling of the potential (scan-rate, 100 mV s^{-1}) over the range −0.20 to +1.20 V vs Ag/AgCl produced a barely detectable

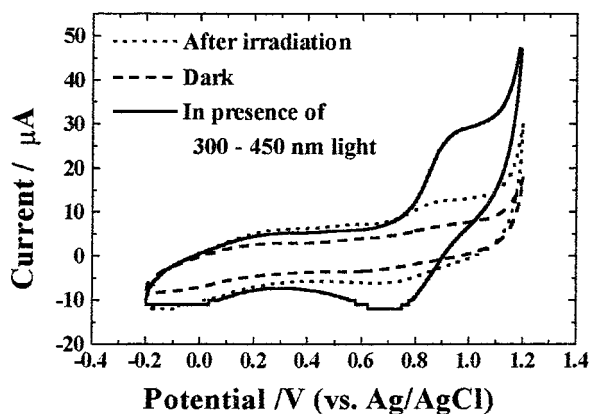(30) Shaw, S. J.; Marken, F.; Bond, A. M. *Electroanalysis* **1996**, *8*, 732.

Figure 1. Solid-state cyclic voltammograms obtained at a scan rate of 100 mV s^{-1} for oxidation of *fac*-Mn(CO)$_3$(η^2-dpm)Cl attached to a pyrolytic graphite electrode and placed in contact with aqueous 0.1 M NaCl electrolyte: (- - -) 10th "dark" cycle, (—) 10th "light" cycle (wavelength, 300−450 nm; intensity, 10 mW cm^{-2}), and (···) 10th "dark" cycle following 10 "light" cycles of the potential.

Figure 2. Phototransient response obtained for the oxidation of solid *fac*-Mn(CO)$_3$(η^2-dpm)Cl attached to a graphite electrode and placed in contact with aqueous (0.1 M NaClO$_4$) electrolyte after irradiation by light of different wavelengths. The electrode was held at a potential of +1.10 V vs Ag/AgCl.

oxidation process at E_p^{ox} = +0.90 V with a corresponding reduction process at E_p^{red} = +0.62 V (Figure 1), where E_p^{ox} and E_p^{red} are oxidation and reduction peak potentials, respectively. Repetitive cycling of the potential (50 cycles) failed to yield any significant improvement in the voltammetric response, relative to that shown in Figure 1. A weak, barely detectable chemically reversible response also is observed at E_p^{ox} = +0.23 V and E_p^{red} = −0.10 V after 10 cycles of the potential. This overall behavior appears to be closely related to the square reaction scheme[26,27] observed in dichloromethane. In organic solvent solution-phase voltammetry, *fac*-Mn(CO)$_3$(η^2-dpm)Cl is oxidized to the 17-electron cationic *fac*$^+$ form which then rapidly isomerizes to the *mer*$^+$ form, which then gives rise to a chemically reversible *mer*$^{+/0}$ couple at a less positive potential. By analogy, in the solid-state situation, the processes with peak potentials of +0.90 and +0.62 V are postulated to be associated with the *fac*-[Mn(CO)$_3$(η^2-dpm)Cl]$^{+/0}$ couple, while the processes at less positive potentials are attributable to the *mer*-[Mn(CO)$_3$(η^2-dpm)Cl]$^{+/0}$ couple, with of course substantially different mechanisms applying to the solution and solid-state voltammetry.

In the presence of 300−450 nm irradiation, the solid-state voltammetry for oxidation of *fac*-Mn(CO)$_3$(η^2-dpm)Cl becomes far better defined (Figure 1). Now, after 10 or more cycles of the potential and using a scan rate of 100 mV s^{-1}, a clearly detected *fac/fac*$^+$ response is observed (E_p^{ox} = +0.98 V; E_p^{red} = +0.71 V), while the peak current associated with the *mer/mer*$^+$ process is only slightly enhanced (E_p^{ox} = +0.23 V, E_P^{red} = −0.10 V). Additional cycling of the potential beyond the first 10 cycles yielded little further change in the voltammetry of *fac*-Mn(CO)$_3$(η^2-dpm)Cl attached to the electrode surface. The photolytic *fac* oxidative peak current enhancement decreased as the scan rate increased, with negligible photoenhancement being observed at scan rates greater than 1 V s^{-1}.

Related results to those described above are observed when the managanese(I) carbonyl compound is attached to a platinum electrode and placed in contact with an aqueous electrolyte (0.1 M NaCl) solution. The peak potentials are now as follows, for *fac/fac*$^+$ E_p^{ox} = +0.91 V and for *mer/mer*$^+$ E_p^{ox} = +0.18 V and E_p^{red} = −0.06 V, but no peak for reduction of *fac*$^+$ could be detected above the background signal.

When the potential of the graphite electrode is more positive than for the *fac* oxidation (+1.10 V), the phototransient response illustrated in Figure 2 is obtained. Under these conditions, the

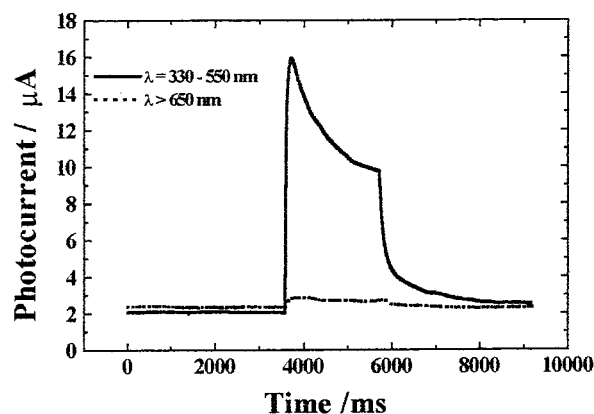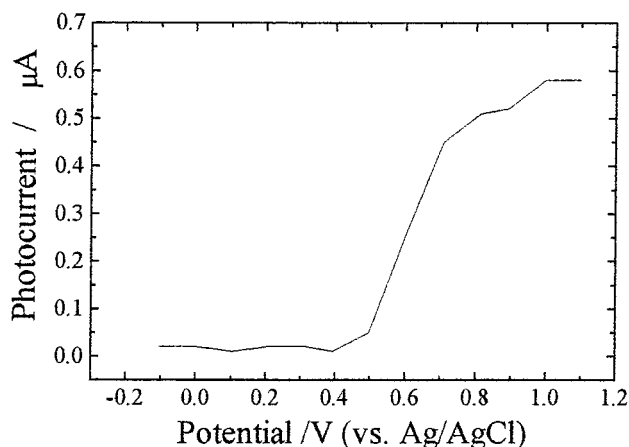**Figure 3.** Dependence of photocurrent on electrode potential for the oxidation of solid *fac*-Mn(CO)$_3$(η^2-dpm)Cl attached to a pyrolytic graphite electrode and placed in contact with 0.1 M NaCl aqueous electrolyte.

current, I, initially rises rapidly and then decays rapidly with time, t, in a Cottrellian manner (I proportional to $t^{-1/2}$) presumably due to a diffusional relaxation process (see later). If the magnitude of the photocurrent is measured as a function of wavelength, using a sequence of colored glass filters, then the maximum value is observed between 350 and 450 nm, with the photocurrent tailing off to zero for wavelengths greater than 500 nm. The wavelength for the maximum photocurrent correlates with the 385 mm charge-transfer absorption spectrum in the electronic spectrum of *fac*-Mn(CO)$_3$(η^2-dpm)Cl. Thus, the photocurrent can be attributed to a process associated with absorption of light by *fac*-Mn(CO)$_3$(η^2-dpm)Cl.

Figure 3 displays the photocurrent associated with the oxidation of *fac*-Mn(CO)$_3$(η^2-dpm)Cl (300−450 nm wavelength light) as a function of applied potential. An increase in photocurrent is observed only over the potential range where oxidation of the *fac*-manganese(I) species occurs

B. Effect of the Nature of the Electrolyte. Table 1 summarizes the data obtained for the solid-state voltammetry of *fac*-Mn(CO)$_3$(η^2-dpm)Cl in the presence of 300−450 nm irradiation when the electrolyte present in the solution phase is varied.

(i) Anion Dependence. For the F$^-$/NO$_3^-$/ClO$_4^-$ series of sodium salts, two processes again are observed upon irradiation with 300−450 nm UV/visible light. However, the potentials are

Table 1. Voltammetric Data Obtained at a Scan Rate of 100 mV s^{-1} When Solid *fac*-Mn(CO)$_3$(η^2-dpm)Cl Attached to a 5 mm Diameter Pyrolytic Graphite Electrode in Contact with 0.1 M Aqueous Electrolyte Solution Is Irradiated with 300 to 450 nm UV/Visible Light (10 mW cm^{-2})[a]

electrolyte	$E_p^{ox}(fac)$/V	$E_p^{red}(fac)$/V	$E_p^{ox}(mer)$/V	$E_p^{red}(mer)$/V	comments
NaCl	0.98	0.71	0.23	−0.10	well-resolved peaks
NaNO$_3$	0.89	0.70	0.26	−0.10	well-resolved peaks
NaF	0.67	0.45	0.45	−0.02	broad *mer* peaks
Na$_2$SO$_4$	0.86/1.05	0.63	0.18/0.35	−0.11	split oxidation peaks
NaClO$_4$	0.98	0.78	0.63	−	broad peaks
KCl	0.97	0.63	0.33	−0.05	well-resolved peaks
BaCl$_2$	0.87	0.57	0.18	−0.05	broad peaks
LiCl	0.89	0.63	0.45	−	well-resolved peaks

[a] Peak potentials are reported from the tenth cycle of the potential in the presence of light.
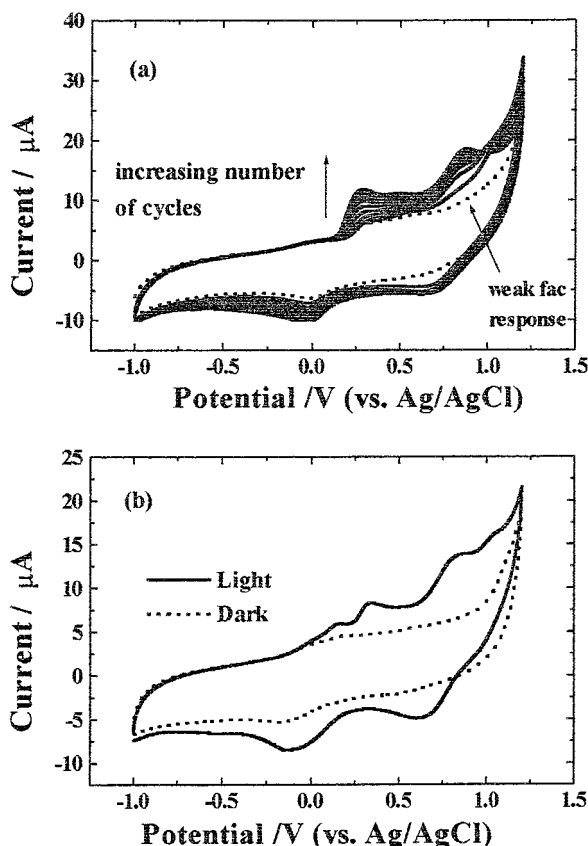

Figure 5. EPR spectra obtained in the ex situ mode at 77 K after *fac*-Mn(CO)$_3$(η^2-dpm)Cl is attached to a graphite electrode (open circuit potential) and then placed in contact with 0.1 M NaCl aqueous electrolyte for 5 min: (lower curve) absence of light and (upper curve) presence of 300−450 nm UV/visible light (intensity, 10 mW cm^{-2}).

Figure 4. First 10 cycles of solid-state cyclic voltammograms obtained at a scan rate of 100 mV s^{-1} for *fac*-Mn(CO)$_3$(η^2-dpm)Cl attached to a pyrolytic graphite electrode and placed in contact with aqueous (a) 0.1 M NaNO$_3$ and (b) 0.1 M Na$_2$SO$_4$ electrolyte following irradiation by 300−450 nm UV/visible light. The initial "light" cycle is represented by a dotted (···) line.

considerably different from those observed when 0.1 M NaCl is present. The dramatic effect of irradiation is shown in Figure 4a when the aqueous medium contains 0.1 M NaNO$_3$. In the initial cycle, the voltammetric responses are very weak, even in the presence of light. However, after 10 cycles of the potential, both reversible oxidation processes are very well defined. In the presence of 0.1 M Na$_2$SO$_4$ as the electrolyte, the *fac* and *mer* oxidation peaks are split (Figure 4b) presumably because either SO$_4^{2-}$ or HSO$_4^-$ may be incorporated into the microcrystalline structure to give different potentials for the Mn-(I) to Mn(II) processes, or two different phases of *fac*- and *mer*-[Mn(CO)$_3$(η^{2-}dpm)Cl]$_2$SO$_4$ exist, each having slightly different potentials.

(ii) Cation Dependence. A series of chloride salts were examined to probe the effect of the cation in the electrolyte.
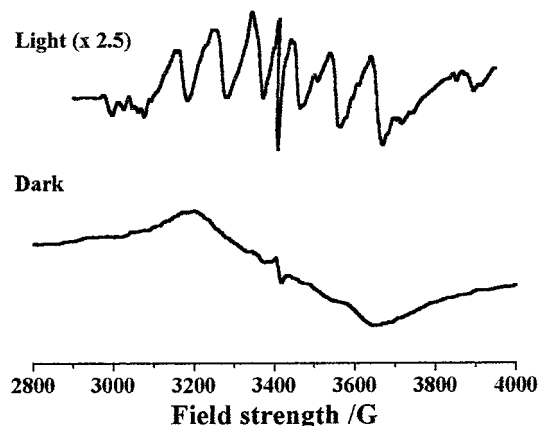
For KCl and LiCl the oxidation potentials are similar to those recorded in 0.1 M NaCl and the photovoltammetric response is similar to that in Figure 1. However, with 0.1 M LiCl as the electrolyte, the *mer*$^+$ reduction peak was only observed at slow scan rates (10 mV s^{-1}). When BaCl$_2$ was used as the electrolyte, well-defined voltammetry also was only observed at slow scan rates (10 mV s^{-1}).

C. EPR and Electron Microprobe Studies. To identify the origin of the photocatalysis, solid *fac*-Mn(CO)$_3$(η^2-dpm)Cl was mechanically attached to the graphite surface. The electrode was then placed in aqueous 0.1 M NaCl at open circuit potential. After 5 min, the electrode was removed from the solution and left to dry. The manganese material was then scraped off the electrode surface and placed in an EPR tube. Figure 5 shows that in the absence of light, a single line EPR response is observed at 3415 G. This signal is associated with the graphite material now present as a mixture with manganese compound (as confirmed by recording the EPR spectrum of the graphite in the absence of any attached manganese compound). In the presence of light, of wavelength 300−450 nm, an additional six-line EPR spectrum is obtained, which is consistent with the formation of an oxidized manganese(II) complex (spin $I = 5/2$). The spectrum shown in Figure 5 is consistent with the presence of high-spin Mn(II). However, because of the relatively high intensity usually associated[31] with isotropic sharp-line spectra obtained with the high-spin state versus the low-intensity broad anisotropic spectra commonly found with the low-spin state, it

(31) (a) Cookson, D. J.; Smith, T. D.; Boas, J. F.; Hicks, P. R.; Pilbrow, J. R. *J. Chem. Soc., Dalton Trans.* **1977**, 211. (b) Carriedo, G. A.; Connelly, N. G.; Perez-Carreno, E.; Orpen, G. A.; Rieger, A. L.; Rieger, P. H.; Riera, V.; Rosair, M. *J. Chem. Soc., Dalton Trans.* **1993**, 3103.
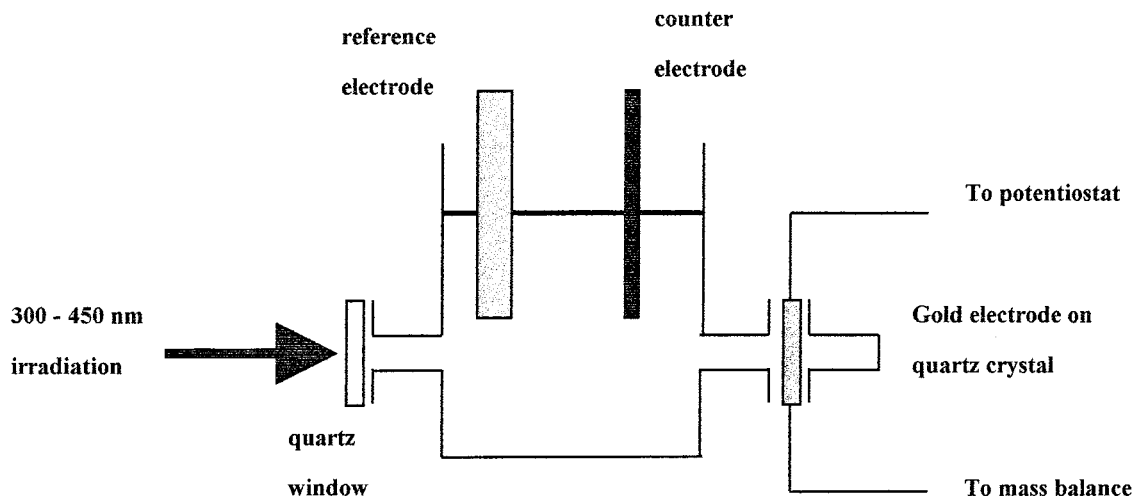
Figure 6. Schematic diagram of the EQCM cell used in photoelectrochemical experiments.

is not possible on the basis of the EPR evidence to exclude the presence of a high concentration of a low-spin manganese(II) complex. Importantly, despite uncertainties in the assignment of the spin state, the EPR result implies that even in the absence of any externally applied potential, the manganese(I) complex attached to the electrode surface in contact with an aqueous (electrolyte) solution phase can be oxidized to a Mn(II) complex upon photolysis. Furthermore, it can be noted that the EPR spectrum also is similar to that observed after chemical oxidation of *fac*-Mn(CO)$_3$(η^2-dpm)Cl.[26,27] The EPR spectra in Figure 5 were obtained at 77 K. At ambient temperature (293 K), EPR spectra were barely detectable above background, but have the same basic features as those observed at 77 K.

Electron microprobe experiments on the nonphotolyzed solid confirmed that the elemental distribution of manganese, chlorine, and phosphorus is in the 1:1:2 proportion expected for the formulation Mn(CO)$_3$(η^2-dpm)Cl. After application of UV/visible light for 5 min, the relative level of chlorine in the solid material attached to the electrode surface, as determined after removal from an electrode placed in 0.1 M NaCl, which was thoroughly rinsed with water, is significantly enhanced by up to 50% whereas the manganese and phosphorus levels always remained in the expected 1:2 ratio. The fact that sodium was not detected confirmed that all NaCl from the electrolyte had been removed by the rinsing procedure. This result suggests that irradiation leads to a photooxidation process which in turn causes chloride anions from the aqueous electrolyte to become incorporated into the manganese(II) microcrystals to form [Mn-(CO)$_3$(η^2-dpm)Cl]Cl on the surface. Thus, both the EPR and microprobe data infer that the manganese(I) species attached to the electrode surface are partially oxidized to the manganese-(II) state upon irradiation. The electron probe data confirm that the chloride anion is transported from the solution to solid phase as a consequence of photooxidation.

D. Electrochemical Quartz Crystal Microbalance Studies. The EPR and electron probe techniques were applied in an ex situ manner. To obtain in situ data, EQCM experiments were conducted using a cell of design shown in Figure 6. Data were obtained from *fac*-Mn(CO)$_3$(η^2-dpm)Cl attached to a gold electrode in contact with 0.1 M NaCl aqueous solution. The electrode was held at a potential of 0.00 V (vs Ag/AgCl) where oxidation of neither *fac*- or *mer*-Mn(CO)$_3$(η^2-dpm)Cl occurs. Phototransient experiments were conducted when 300−450 nm irradiation (intensity 10 mWcm^{-2}) was focused periodically on the electrode surface.
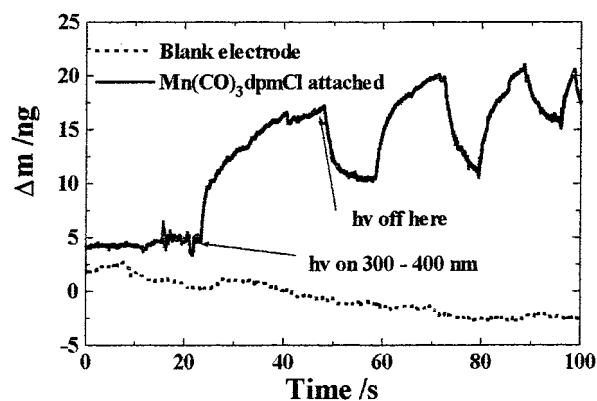

Figure 7. EQCM data obtained when solid *fac*-Mn(CO)$_3$(η^2-dpm)Cl, attached to a gold-coated quartz crystal and placed in contact with aqueous 0.1 M NaCl electrolyte, is irradiated periodically with 300−450 nm light.

Figure 7 shows that an increase in mass is recorded upon irradiation of *fac*-Mn(CO)$_3$(η^2-dpm)Cl attached to the gold electrode surface, while upon terminating the irradiation of the electrode surface, the mass decreases. Upon each subsequent irradiation burst, the mass increases further, with the background dark mass also becoming greater on the time scale of the switching employed in Figure 7. Results contained in Figure 7 confirm that no mass changes occur upon irradiation of a blank gold electrode to which no solid compound has been attached. These in situ EQCM experiments provide further evidence that irradiation of the manganese material is accompanied by anions being incorporated into the structure (increase in mass) which is as expected if photooxidation to a Mn(II) cation occurs.

E. Voltammetry of *fac*-Mn(CO)$_3$(η^2-dpm)Cl Doped with the *mer*-Mn(CO)$_3$(η^2-dpm)Cl]BF$_4$. The above results lead to the conclusion that with irradiation of *fac*-Mn(CO)$_3$(η^2-dpm)-Cl attached to the electrode surface, the rate of transport of electrons and ions within the solid is greatly enhanced via incorporation of a manganese(II) salt. This doping is assumed to increase the conductivity of nonconducting organometallic species (resistivity typically $\geq 10^9$ Ωcm^{17}) and thereby enhance transport of charge to and from the electrode surface via an "electron-hopping" mechanism.[1] This doping mechanism is believed to be the origin of the photocatalysis observed in the solid-state voltammetry of *fac*-Mn(CO)$_3$(η^2-dpm)Cl. If this

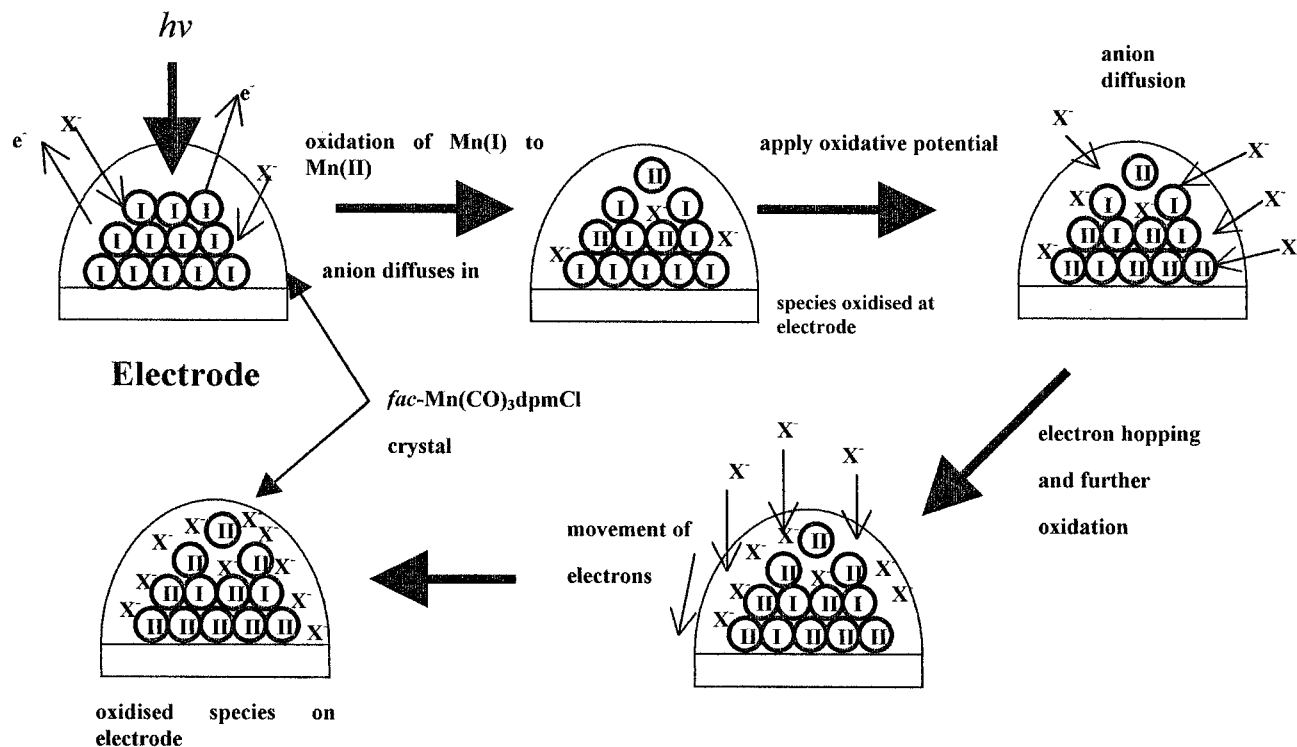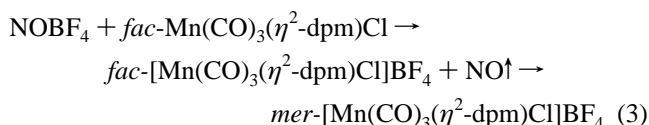(32) Cotton, F. A.; Wilkinson, G. *Advanced Inorganic Chemistry*; John Wiley: New York, 1988.

Figure 8. Mechanism proposed to explain the photocatalysis of the electrochemical oxidation process at the *fac*-Mn(CO)$_3$(η^2-dpm)Cl−electrode−aqueous electrolyte interface.

mechanism is correct, it would be predicted that chemical doping of the solid with an oxidized manganese(II) form of the compound also would lead to current enhancement in the solid-state voltammetry of *fac*-Mn(CO)$_3$(η^2-dpm)Cl.

Chemical doping of *fac*-Mn(CO)$_3$(η^2-dpm)Cl with *mer*-Mn-(CO)$_3$(η^2-dpm)Cl may be achieved as follows. A 10 mM dichloromethane solution of *fac*-Mn(CO)$_3$(η^2-dpm)Cl was prepared to which small molar quantities of the one-electron oxidant NOBF$_4$[32] was added to generate *mer*-manganese(II) tetrafluoroborate salt via the oxidation-isomerization[26,27] reaction:

$$NOBF_4 + fac\text{-}Mn(CO)_3(\eta^2\text{-}dpm)Cl \rightarrow$$
$$fac\text{-}[Mn(CO)_3(\eta^2\text{-}dpm)Cl]BF_4 + NO\uparrow \rightarrow$$
$$mer\text{-}[Mn(CO)_3(\eta^2\text{-}dpm)Cl]BF_4 \quad (3)$$

Doping levels up to the 10% level were achieved via this method. One milliliter of the resulting dichloromethane solution mixture of the *fac*-Mn(CO)$_3$(η^2-dpm)Cl and *mer*-[Mn(CO)$_3$(η^2-dpm)Cl]BF$_4$ was then placed on the surface of a freshly cleaved pyrolytic graphite electrode surface. After evaporation of the solvent, the required solid mixture was deposited onto the electrode surface, and the voltammetric properties were probed. For purposes of comparison, *fac*-Mn(CO)$_3$(η^2-dpm)Cl that had not been doped with its cationic form also was attached to the electrode after evaporation from a dichloromethane solution.

A substantial effect in the voltammetry was observed after doping of *fac*-Mn(CO)$_3$(η^2-dpm)Cl with 5% of the manganese-(II) cation. Thus, for the doped sample and in the dark, a well-defined *fac*-Mn(CO)$_3$(η^2-dpm)Cl oxidation process was observed on the first oxidative voltammetric scan (scan rate, 100 mV s^{-1}), and upon successive oxidative voltammetric scans, a positive shift in the peak potential of the *fac*-Mn(CO)$_3$(η^2-dpm)-Cl oxidation process also occurred as is the case with the photocatalysis experiments described previously. In the experiments described above, presumably microcrystals of both Mn-
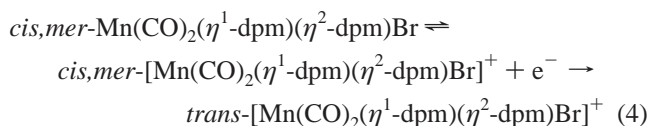
(I) and Mn(II) are formed, each being doped on the surface with small amounts of material in the other oxidation state, in a manner akin to that achieved by photooxidation of *fac*-Mn-(CO)$_3$(η^2-dpm)Cl.

F. Mechanism of the Photocatalysis of the Solid-State Voltammetry. The combination of results obtained by EPR, electron microprobe, EQCM, and chemical doping experiments suggest that irradiation of *fac*-Mn(CO)$_3$(η^2-dpm)Cl attached to an electrode surface in contact with 0.1 M NaCl electrolyte results in photooxidation of the manganese(I) compound to a manganese(II) cation with concomitant injection of chloride anions from the electrolyte occurring to neutralize the excess positive charge generated.

Figure 8 represents a schematic diagram of a mechanism proposed to explain the photocatalysis. It is suggested that upon photolysis of the microcrystalline material, the manganese(I) species forms a charge-transfer excited state, which is then rapidly oxidized to a *fac*-manganese(II) cationic product that can then isomerize to the *mer*$^+$ form. From solution-phase studies, it is known that photolysis of *fac*-Mn(CO)$_3$(η^2-dpm)Cl induces isomerization to the *mer* form.[26,27] Thus, it is also possible that it is this *mer* isomer generated by photoisomerization that is in turn photooxidized directly to its *mer* cationic form. Presumably, reduction of water at the interface and transfer of chloride ion from the electrolyte to solid phases complete the photoredox reaction. Voltammetric evidence for the formation of the *mer* isomeric form upon photolysis is provided by the fact that a *mer*$^{+/0}$ couple is observed in initial cycles in the presence of light at a less positive potential than that for oxidation of the *fac* isomer (see Figure 1, 4, and 5). Photooxidation and charge neutralization results in the holes of Mn(II) being created at the surface. The *mer*$^+$ doped material is now in a better state to transport charge when oxidation of the *fac*-Mn(CO)$_3$(η^2-dpm)Cl occurs at the solid−electrode interface and thus photocatalysis of the current occurs upon electronic excitation of the material attached to the electrode surface.

Phototransient experiments (Figure 2) therefore are analogous to switching on the oxidizing power of the electrode via a potential step to an appropriate potential and observing the current decay due to mass transport processes associated with anion diffusion.

If the above ideas are correct, then other compounds having properties related to *fac*-Mn(CO)$_3$(η^2-dpm)Cl also should exhibit voltammetric photocatalysis. The solid-state photovoltammetry of *cis,mer*-Mn(CO)$_2$(η^1-dpm)(η^2-dpm)Br adhered to an electrode in contact with 0.1 M aqueous NaCl was therefore examined. The organic solvent solution-phase voltammetry[33] of interest for this species consists of the one-electron oxidation process,

$$cis,mer\text{-}Mn(CO)_2(\eta^1\text{-dpm})(\eta^2\text{-dpm})Br \rightleftharpoons$$

$$cis,mer\text{-}[Mn(CO)_2(\eta^1\text{-dpm})(\eta^2\text{-dpm})Br]^+ + e^- \longrightarrow$$

$$trans\text{-}[Mn(CO)_2(\eta^1\text{-dpm})(\eta^2\text{-dpm})Br]^+ \quad (4)$$

A *cis-fac*-[Mn(CO)$_2$(η^1-dpm)(η^2-dpm)Br]$^+$ intermediate may also be relevant to the isomerization reaction in eq 4. It can be seen from Figure 9 that significant photocatalysis is observed for electrochemical oxidation of *cis,mer*-Mn(CO)$_2$(η^1-dpm)(η^2-dpm)Br in the presence of 300−450 nm UV/visible irradiation, the wavelength of which corresponds to a *cis,mer*-Mn(CO)$_2$-(η^1-dpm)(η^2-dpm)Br charge-transfer band (λ_{max} = 398 nm in acetonitrile solution).

Conclusions

The voltammetry of poorly conducting solids attached to electrode surfaces that are in contact with a solvent (electrolyte)

(33) Eklund, J. C.; Bond, A. M.; Colton, R.; Humphrey, D. G.; Mahon, P. J.; Walter, J. N. *Inorg. Chem.* **1999**, *38*, 2005.
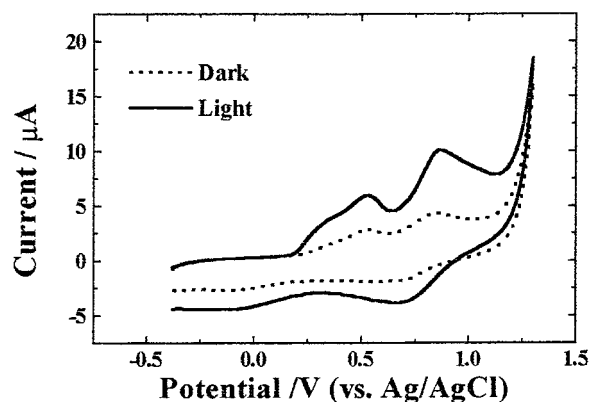

Figure 9. Solid-state voltammograms obtained in the presence and absence of 300−450 nm UV/visible irradiation when *cis,mer*-Mn(CO)$_2$-(η^1-dpm)(η^2-dpm)Br is attached to a pyrolytic graphite electrode and then placed in contact with an aqueous 0.1 M NaCl electrolyte. Initial cycle shown at a scan rate of 100 mV s^{-1}.

may be catalyzed if irradiation with light of a wavelength corresponding to an absorption band can induce a suitable doping mechanism. This possibility has been demonstrated in the case of photoactive manganese carbonyl complexes which can exist in two readily accessible oxidation states and two isomeric forms having different reversible potentials.